

W 81.

# An Adaptive Domain Decomposition Procedure for Boltzmann and Euler Equations

S. Tiwari

Fachbereich Mathematik, Universität Kaiserslautern  
Kaiserslautern, Germany

A. Klar

Fachbereich Mathematik, Universität Kaiserslautern  
Kaiserslautern, Germany

## Abstract

In this paper we present a domain decomposition approach for the coupling of Boltzmann and Euler equations. Particle methods are used for both equations. This leads to a simple implementation of the coupling procedure and to natural interface conditions between the two domains. Adaptive time and space discretizations and a direct coupling procedure lead to considerable gains in CPU time compared to a solution of the full Boltzmann equation. Several test cases involving a large range of Knudsen numbers are numerically investigated.

**Keywords.** domain decomposition, particle methods, kinetic equations, fluid dynamic equations, adaptive grid generation

## 1 Introduction

Boltzmann- and fluid dynamic equations (such as Euler or Navier-Stokes equations) are used to model hypersonic gas flows. Numerical simulations of such flows are useful for example in the design of space vehicles, in particular, in understanding the behavior of the early phases of reentry flights.

Such flows are usually far from any kind of local equilibrium states. This means that variants of the Boltzmann equation have to be used as first principle equations instead of fluid dynamic equations. However, when the mean free path of molecules becomes small - for example during the reentry - standard numerical methods for the Boltzmann equation become exceedingly expensive in computing time. Therefore, gas dynamics equations should be used if possible, i.e. in other words, near local equilibrium states and outside of shock and boundary layers. These considerations

prompt the use of domain decomposition strategies, where the Boltzmann equation is to be solved only in regions others than those mentioned above.

Essentially three problems have to be solved in order to compute a solution of the domain decomposition problem: First one has to choose suitable codes for Boltzmann and Euler equations. Second, the regions, where the fluid dynamic equations can be used, have to be determined. Once this is done the third problem is the matching of the Boltzmann code with the Euler or Navier- Stokes solver. We refer to [18, 17, 5, 4, 21, 11, 13, 14, 28] for different domain decomposition approaches. In this paper Boltzmann and Euler equations are solved by particle methods. Numerical codes for the Boltzmann equation are usually based on particle methods, see [1, 2, 3, 23]. Although for the Euler equations a variety of other methods exist, we did choose for the domain decomposition approach a particle method as well, since they are particularly suited for the coupling to the Boltzmann code. To determine the equilibrium or Euler domains automatically we use an approach derived from Grad's thirteen moment ansatz, see [27, 26, 15]. The two equations are coupled together by a natural condition guaranteeing the equality of fluxes at the interface. Moreover, we use an adaptive grid refinement procedure for the spatial and temporal discretization. The refinement is adapted to the stability requirements on the time step in each of the domains.

The main focus of the present paper is a study of the coupled solution for the whole range of mean free paths and of the possible gain in CPU time, which depends strongly on the size of the mean free path. In particular, the use of an adaptive time and space discretization in the two domains yields a considerable gain in CPU time. CPU time is shown to be smaller by a factor 10 and more compared to a full Boltzmann solution for certain situations and ranges of the mean free path.

The paper is organized in the following way: Section 2 describes shortly the equations to be coupled and the numerical codes to solve them. Section 3 describes in more detail the coupling algorithm. Section 4 gives a presentation of our numerical results and a comparison of the CPU times for different Knudsen numbers.

## 2 Equations and Numerical Methods

### 2.1 Equations

The Boltzmann equation describes the time evolution of a distribution function  $f(t, x, v)$  for particles of velocity  $v \in \mathbb{R}^3$  at point  $x \in D \subset \mathbb{R}^d$  and time  $t \in \mathbb{R}_+$ . It is given by

$$\frac{\partial f}{\partial t} + v \cdot \nabla_x f = \frac{1}{\epsilon} J(f, f), \quad (1)$$

where the Knudsen number  $\epsilon$  is proportional to the mean free path and

$$J(f, f) = \int_{\mathbb{R}^3} \int_{S^2} k(|v-w|, \eta) [f(v')f(w') - f(v)f(w)] d\omega(\eta) dw$$

with

$$v' = T_{v,w}(\eta) = v - \eta \langle \eta, v-w \rangle, w' = T_{w,v}(\eta).$$

For more details we refer to [9]. For  $\epsilon$  tending to 0, i.e. for small mean free paths, one can prove [7] that the Boltzmann distribution function  $f$  tends to a local Maxwellian

$$f_M[\rho, u, T](t, x) = \frac{\rho}{(2\pi RT)^{3/2}} e^{-\frac{|v-u|^2}{2RT}}, \quad (2)$$

where the parameters  $\rho, u, T(t, x)$  are given by the solution of the compressible Euler equations:

$$\begin{aligned} \frac{\partial \rho}{\partial t} + \nabla_x \cdot (\rho u) &= 0 \\ \frac{\partial}{\partial t}(\rho u) + \nabla_x \cdot (\rho u \otimes u) + \nabla_x(\rho RT) &= 0, \\ \frac{\partial}{\partial t}(\rho(\frac{1}{2}u^2 + \frac{3}{2}RT)) + \nabla_x \cdot (\rho u(\frac{1}{2}u^2 + \frac{5}{2}RT)) &= 0. \end{aligned} \quad (3)$$

We solve Boltzmann- and Euler equations by particle method. The methods are described in 2.2 and 2.3 respectively.

## 2.2 Particle Method for the Boltzmann equation

The solution method for the Boltzmann equation is explained in detail in [2] or [23]. It is based on the time splitting of the equation. Introducing fractional steps one solves first the free transport equation in  $[0, \Delta t]$ :

$$\frac{\partial f}{\partial t} + v \cdot \nabla_x f = 0. \quad (4)$$

If the particle approximation of the initial value  $f(0, x, v)$  of (4) is given by some discrete measure  $\sum_{j=1}^N \alpha_j \delta_{(x_j, v_j)}$ , then the time evolution of this particle ensemble is simply

$$\sum_{j=1}^N \alpha_j \delta_{(x_j + tv_j, v_j)}.$$

During the free flow boundary and interface conditions are taken into account.

In a second step the homogeneous Boltzmann equation

$$\frac{\partial f}{\partial t} = \frac{1}{\epsilon} J(f, f) \quad (5)$$

is solved. To simulate equation (5) by a particle method an explicit Euler step is used and equation (5) is written in the discretized form

$$f(\Delta t, v) = f(0, v) + \frac{\Delta t}{\epsilon} J[f, f](0, v). \quad (6)$$

$f(\Delta t, v)$  is then used in the next time step as the new initial condition for the free flow. One considers equation (6) in a weak formulation, i. e.

$$\begin{aligned} & \int \Phi(v) f(\Delta t, v) dv \\ &= \int_{\mathbb{R}^3} \int_{\mathbb{R}^3} \int_{S^2} \left[ \frac{\Delta t}{\epsilon} k \Phi(v') + \left(1 - \frac{\Delta t}{\epsilon} k\right) \Phi(v) \right] d\omega(n) f(0, v) f(0, w) dw dv \end{aligned} \quad (7)$$

for test functions  $\Phi$ . To solve equation (7) we need an approximation of the product measure

$$d\omega(n) f(0, v) f(0, w) dw dv$$

by some  $\sum_{j=1}^N \alpha'_j \delta_{(n_j, v_j, w_j)}$ , given only an approximation  $\sum_{j=1}^N \alpha_j \delta_{v_j}$  of  $f(0, v) dv$ . If this problem is solved and  $\sum_{j=1}^N \alpha'_j \delta_{(n_j, v_j, w_j)}$  is determined, one can compute the time evolution of the measure due to (7): The factor  $1 - \frac{\Delta t}{\epsilon} k$  is interpreted as a probability for a dummy collision, keeping the old velocities.  $\frac{\Delta t}{\epsilon} k$  is the probability for a real collision, changing  $v_j \rightarrow v'_j = T_{v_j, w_j}(\eta_j)$ . For more details about the solution procedure for the space homogeneous Boltzmann equation we refer to the above cited references.

One observes that, to guarantee the positivity of the function  $f(\Delta t, v)$ , we need the following restriction on the time step

$$1 - \frac{\Delta t}{\epsilon} k \geq 0. \quad (8)$$

This means that for  $\epsilon \rightarrow 0$  the time step  $\Delta t$  has to be shrunk with  $\epsilon$ , the equations are becoming stiff. The method becomes exceedingly expensive for small Knudsen numbers.

### 2.3 Particle method for solving the Euler equation

For small Knudsen numbers  $\epsilon$  and outside of shock and boundary layers the solution of the Euler equations is a good alternative to the solution of the full Boltzmann problem. In these regimes the solution of the kinetic problem is approximated by the Euler equations with good accuracy. Moreover, to obtain stability for the Euler

equations one does not need to fulfill the restrictive condition (8), but only the usual CFL condition for Euler equations.

We solve the Euler equations by a particle method based on kinetic schemes. Here, we give only a short description of the method which will be used in the calculation and refer to [10], [16], [24], [25] for further details about kinetic schemes and particle methods based on kinetic scheme.

One defines the macroscopic quantities  $\rho, \rho u, T$  as the moments of a distribution function  $f(t, x, v)$ :

$$\begin{aligned}\rho &= \int_{\mathbb{R}^3} f(t, x, v) dv \\ u &= \frac{1}{\rho} \int_{\mathbb{R}^3} v f(t, x, v) dv \\ \frac{|u|^2}{2} + \frac{3}{2} RT &= \frac{1}{\rho} \int_{\mathbb{R}^3} \frac{|v|^2}{2} f(t, x, v) dv.\end{aligned}$$

Then one tries to find a simple evolution for the density  $f$  such that this evolution approximates the compressible Euler equations for  $\rho, \rho u, T$ . This evolution consists of two steps as in the Boltzmann case. In each time step we proceed as follows:

First, a simple free flow is performed, i.e. we solve:

$$\frac{\partial f}{\partial t} + v \cdot \frac{\partial f}{\partial x} = 0.$$

The particle approximation is done as in the Boltzmann case.

Second a projection onto an equilibrium distribution function  $G = G[\rho, u, T](v)$ , which is uniquely defined by the first five moments, is performed. The projection is given by computing the moments  $\rho, u, T$  of  $f$  and determining the associated equilibrium function  $G[\rho, u, T](v)$ . The resulting function is then used as the initial distribution for the next free flow step. The particle approximation of the projection step is done by calculating the moments  $\rho, u, T$  of the particle distribution after the free flow evolution. The particles are then generated again according to the new equilibrium distribution  $G[\rho, u, T]$ . The class of equilibrium distribution functions  $G$  is chosen in such a way that the approximation of the Euler evolution is guaranteed. We consider an equilibrium class of the form

$$G[\rho, u, T](v) = \frac{\rho}{(RT)^{3/2}} \chi\left(\frac{v-u}{\sqrt{RT}}\right), \quad (9)$$

where  $\chi : \mathbb{R}^3 \rightarrow \mathbb{R}^3$  is an integrable function with

$$\chi(\xi) = \chi(-\xi), \quad \int_{\mathbb{R}^3} \chi(\xi) d\xi = 1, \quad \int_{\mathbb{R}^3} \xi_i^2 \chi(\xi) d\xi = 1.$$

### **Example 1**

Let  $\chi(\xi) = \left(\frac{1}{2\pi}\right)^{3/2} e^{-\frac{|\xi|^2}{2}}$ , then  $G[\rho, u, T](v)$  is a Maxwellian distribution of the form (2).

### **Example 2**

Define  $\chi(\xi) = \frac{3}{4\pi(5)^{\frac{3}{2}}} \cdot 1_{B_{\sqrt{5}}}(\xi)$ , where  $1_{B_{\sqrt{5}}}$  denotes the characteristic function of the ball in  $\mathbb{R}^3$  with radius  $\sqrt{5}$ . This gives the Kaniel equilibrium distribution for monatomic gas introduced in [16].

## **3 The Domain Decomposition Algorithm**

In this section we describe the coupling algorithm in more detail. To compute an approximation of the stationary solution of the Boltzmann problem by a direct coupling procedure we proceed in the following way:

In each time step Boltzmann and Euler domains are determined using a criterion described in subsection 3.1. This leads to a separation of the computational domain  $D$  into a Boltzmann domain  $D_B$  and an Euler domain  $D_E$ . To obtain suitable boundary conditions at the interface between the two domains, the equations are coupled together in a natural way: The use of a particle method based on a kinetic scheme for the Euler equations leads to coupling conditions based on the equality of fluxes at the interface. This is described in (3.2). Boltzmann and Euler equations are then solved for one time step in their respective domains by the methods described in section 2 taking coupling and boundary conditions into account.

To save CPU time by the coupling procedure the essential point is to use a space and time discretization which is adapted to the stiffness of the problem. These aspects are described in section (3.3).

### **3.1 Criteria of local equilibrium**

As discussed above, the Euler equations are valid if the Boltzmann distribution function is near to a local equilibrium distribution of the form (2). Therefore, a test is needed whether the particle distribution is close to a Maxwellian or not.

To obtain a criterion the distribution function  $f(t, x, v)$  is written in the form

$$f = f_M(1 + \phi), \tag{10}$$

where  $f_M$  is the local Maxwellian with first five moments  $\rho, u$  and  $T$  equal to those of  $f$ .  $\phi$  denotes the deviation from the equilibrium, see [8]. The size of  $\phi$  is then

estimated with an appropriate norm  $\|\cdot\|$ . Local thermal equilibrium can be assumed if  $\|\phi\| \ll 1$ . Kinetic theory suggests to define a Hilbert space, where the scalar product is defined by [8]

$$\langle \phi, \psi \rangle = \int_{\mathbb{R}^3} \frac{f_M}{\rho} \phi \psi dv. \quad (11)$$

The first five moments of  $f$  are those of  $f_M$ , i.e.

$$\int_{\mathbb{R}^3} \phi f_M dv = 0, \quad (12)$$

$$\int_{\mathbb{R}^3} v \phi f_M dv = 0, \quad (13)$$

$$\int_{\mathbb{R}^3} |v|^2 \phi f_M dv = 0. \quad (14)$$

One defines the heat flux

$$q = \frac{1}{2} \int_{\mathbb{R}^3} (v - u) |v - u|^2 f dv$$

and the stress tensor

$$\tau = \int_{\mathbb{R}^3} (v - u) \cdot (v - u)^T f dv - \rho RT I$$

with the identity matrix  $I$ . Heat flux and stress tensor of a local Maxwellian distribution are 0. Therefore

$$\frac{1}{2} \int_{\mathbb{R}^3} (v - u) |v - u|^2 \phi f_M dv = q \quad (15)$$

and

$$\int_{\mathbb{R}^3} (v - u) \cdot (v - u)^T \phi f_M dv = \tau. \quad (16)$$

The non-vanishing of the symmetric stress tensor  $\tau$  and of the heat flux vector  $q$  is due to the deviation of the distribution function from a Maxwellian distribution.

With the help of the above thirteen equations (12)-(16) we express  $\phi$  as a polynomial: Following Grad [12] we make the ansatz

$$\phi = a + b \cdot (v - u) + (v - u)^T \cdot C \cdot (v - u) + d \cdot (v - u) |v - u|^2, \quad (17)$$

where  $a$  is a scalar,  $b, d$  are vectors in  $\mathbb{R}^3$  and  $C$  is a  $(3 \times 3)$  symmetric matrix.

Now, all coefficients of the polynomial (17) are determined with the help of (12)-(16) by substituting  $\phi$ . We obtain with  $\tau = (\tau_{ij})$

$$\begin{aligned} \phi &= \frac{q \cdot (v - u)}{\rho(RT)^2} \left[ \frac{|v - u|^2}{5RT} - 1 \right] \\ &+ \frac{1}{2\rho(RT)^2} \left[ \tau_{11}(v_1 - u_1)^2 + \tau_{22}(v_2 - u_2)^2 - (\tau_{11} + \tau_{22})(v_3 - u_3)^2 \right] \\ &+ \frac{1}{\rho(RT)^2} \left[ \tau_{12}(v_1 - u_1)(v_2 - u_2) + \tau_{23}(v_2 - u_2)(v_3 - u_3) \right] \\ &+ \frac{1}{\rho(RT)^2} \tau_{13}(v_1 - u_1)(v_3 - u_3). \end{aligned} \quad (18)$$



A short calculation gives

$$\|\phi\| = \frac{1}{\rho RT} \left[ \frac{2}{5} \frac{|q|^2}{RT} + \frac{1}{2} \|\tau\|_E^2 \right]^{1/2}, \quad (19)$$

where  $\|\tau\|_E$  is the Euclidean norm of the stress tensor matrix.  $\|\phi\|$  gives a criterion of equilibrium, which identifies the Boltzmann and Euler cells during the simulation. Heat flux vector and stress tensor have to vanish in order to yield the closure relations for the Euler equations. If  $\|\phi\|$  is small compared to unity, the particle system is close to a Maxwellian distribution. Otherwise, it is far away from it.

We mention that if we do not take into account the stress tensor and consider only the heat flux vector then the present ansatz turns out to be equivalent to the criterion of local thermal equilibrium used by Kreuzer, Meixner, Boyd et al. [19, 6, 22]. Similarly, if we neglect the effect of the heat flux vector in (19), then a criterion similar to the one used by Leipmann et al. [20] is obtained.

In our experience, taking into account only the heat flux vector or only the shear stress tensor, one does not obtain a good criterion. For example, to capture the nonequilibrium domain in the shock region, the consideration of the heat flux vector is sufficient. However, on the boundary and in the wake the shear stress is significant. Finally, we mention that since we solve both Boltzmann and Euler equations by a particle method, one can compute heat flux vector and stress tensor easily for both equations. In particular, a nonvanishing heat flux and stress tensor can also be obtained in the Euler cells after performing the free flow step.

The above criterion yields domains which depend on the Knudsen number. For  $\epsilon$  large, a large Boltzmann domain is obtained, whereas for very small  $\epsilon$  the Boltzmann domain is essentially reduced to a small shock and boundary layer. See Figure 1 for an example.

### 3.2 Coupling conditions

The coupling conditions for the two equations at the interface between Boltzmann and Euler domain are given by the following:

Consider the Boltzmann and Euler domains  $D_B$  and  $D_E$ . Let  $n$  denote the normal at the interface  $I$  between  $D_B$  and  $D_E$  pointing into the Boltzmann domain  $D_B$ . After the projection step in the kinetic scheme we have the following situation: The boundary condition for the free flow equation for the distribution function  $f_E$  in the kinetic scheme in  $D_E$  is given by

$$f_E(t, x, v) = f_B(t, x, v), \quad v \cdot n < 0 \quad (20)$$



for  $x \in I$ . Since the distribution function in the Euler domain is an equilibrium distribution, the outgoing function is an equilibrium distribution. Therefore, we can compute the flux at the boundary as

$$\begin{aligned}
& \int v \cdot n \begin{pmatrix} 1 \\ v \\ \frac{|v|^2}{2} \end{pmatrix} f_E(v) dv \\
&= \int_{v \cdot n < 0} v \cdot n \begin{pmatrix} 1 \\ v \\ \frac{|v|^2}{2} \end{pmatrix} f_B(v) dv \\
&+ \int_{v \cdot n > 0} v \cdot n \begin{pmatrix} 1 \\ v \\ \frac{|v|^2}{2} \end{pmatrix} G(\rho, u, T)(v) dv.
\end{aligned} \tag{21}$$

Since after the projection step the distribution function is in equilibrium in the Euler cells, the above fluxes are equal at the boundary to the fluxes of the Euler equations computed in the kinetic scheme, i.e.

$$\begin{aligned}
& \int_{v \cdot n < 0} v \cdot n \begin{pmatrix} 1 \\ v \\ \frac{|v|^2}{2} \end{pmatrix} f_B(v) dv \\
&+ \int_{v \cdot n > 0} v \cdot n \begin{pmatrix} 1 \\ v \\ \frac{|v|^2}{2} \end{pmatrix} G(\rho, u, T)(v) dv \\
&= \int v \cdot n \begin{pmatrix} 1 \\ v \\ \frac{|v|^2}{2} \end{pmatrix} G(\rho, u, T)(v) dv
\end{aligned} \tag{22}$$

where  $\rho, u, T$  are the solutions of the Euler equations. This is the equality of fluxes at the boundary. We mention that the above considerations are equivalent to the consideration of the half range fluxes for  $v \cdot n < 0$ . In this way we obtain conditions at the interface for the Euler equations. In turn the ingoing function for the Boltzmann region is given by the outgoing function of the Euler region:

$$f_B(x, v, t) = G(\rho, u, T), v \cdot n > 0. \tag{23}$$

The above conditions are naturally realized in the particle scheme. The particles are simply transferred from Boltzmann to Euler cells or vice versa in the free flow step, keeping their velocities. Then they are handled by the projection and collision procedure, respectively. This has to be adapted, if different time steps and grid sizes are used.

### 3.3 Choice of time step and adaptive grid refinement

An adaptive time step and choice of the spatial grid is essential to gain CPU time. Using the same grid and step size in both domains one does not obtain a major gain in CPU time. Instead one has to take into account the stability criterion in a proper way.

The size of the time step for the Boltzmann equation is given by (8), i.e. in particular by the value of the Knudsen number. As mentioned above, in order to gain CPU time one has to use the possibility of choosing a larger time step for the Euler equations: The time step for the Euler equations is only governed by accuracy requirements and the CFL condition and does not depend on the Knudsen number. These considerations lead to the use of small time steps in the Boltzmann domain according to the value of the mean free path. In contrast, in the Euler domain larger time steps are used. We mention that the choice of different time discretization in the two domains leads to the implementation of an inner time loop for the Boltzmann equation for each Euler time step.

For the Boltzmann region the spatial grid size has to be chosen according to the values of the mean free path. Since the solution in the Euler domain is only varying slowly in space (on a macroscopic time scale) the use of coarser grids in the Euler domain is appropriate. In other words the space discretization is chosen for both equations according to the time discretization. An example of such a grid structure is shown in Figure 2.

Using now the same total number of particles for all calculations in the computational domain one can observe how much CPU time is gained by the adaptive choice of the time step. In this case CPU time is only gained by using the time step appropriate to the stability requirements and not by a reduction of the number of particles. See Table 1 for a comparison of the CPU time.

A further gain in CPU time is achieved by using the difference in the spatial grid size in Boltzmann and Euler domain. To obtain approximately the same velocity discretization - which is determined by the number of particles per cell - we use on the average in each spatial cell no matter whether it is Euler or Boltzmann the same number of particles. This is achieved by determining the total number of particles from the number of cells used in the calculation. It leads to a strong reduction of particles for flows with larger Euler domain, i.e. flows with small Knudsen numbers, compared to a full Boltzmann solution. A further gain in CPU time is obtained in this way, see Table 2.

## 4 Numerical results

We consider the hypersonic flow of monatomic gas around an ellipse. The Boltzmann equation (1) is solved with the initial condition

$$f(0, x, v) = \frac{\rho_\infty}{(2\pi RT_\infty)^{3/2}} e^{-\frac{|v-u_\infty|^2}{2RT_\infty}}. \quad (24)$$

The boundary condition is given by an ingoing function of the form

$$f(t, x, v) = \frac{\rho_\infty}{(2\pi RT_\infty)^{3/2}} e^{-\frac{|v-u_\infty|^2}{2RT_\infty}} \quad (25)$$

at the left boundary of the domain  $D$  and absorbing boundary conditions on the other outer boundaries. On the boundary of the ellipse we use diffuse reflection with thermal accomodation as boundary conditions.

The input parameters are the following: at infinity the characteristics of the flow are  $u_\infty = 4126m/sec$ ,  $T_\infty = 200K$  and gas constant  $R = 208Jkg/K$ , which corresponds to a Mach number 15. The temperature of the body is  $1000K$ . The angle of attack is equal to  $30^0$ . The major and minor axes of the ellipse are 1 m and 0.5 m, respectively.

We perform all calculations (full Boltzmann, hybrid code and Euler code) using in one series of comparisons the same total number of particles. In another series we perform calculations with approximately the same number of particles in each cell. The second series yields the correct comparison of the CPU times due to the statements in subsection 3.3.

The value of  $\|\phi\|$  is computed straightforwardly for Boltzmann and Euler cells using the particle approximations of the distribution functions. As a criterion of local equilibrium we assume that, if  $\|\phi\|$  is less than a small number  $\delta$  in each cell, then we denote this cell an Euler cell, otherwise it is a Boltzmann cell. Then collisions in Boltzmann cells and a projection onto the Kaniel or Maxwell distribution in the Euler cells are done. We mention that a kinetic scheme based on the projection onto the Maxwellian fits better to the above described criterion to determine the equilibrium domains. However, the projection onto Kaniel is faster.

We perform the above process in every cell and at every time step. During the simulation of one Euler time step a number of Boltzmann time steps has to be performed in an inner loop.

At the begining all cells are Euler cells. When time advances the Boltzmann and Euler domains separate automatically, leading to Figure 1 below for the final stationary states. The smaller the Knudsen number the smaller is the Boltzmann domain. Finally the Boltzmann equation is only solved in a small shock and boundary layer. This means that for small Knudsen numbers the code is essentially an Euler solver

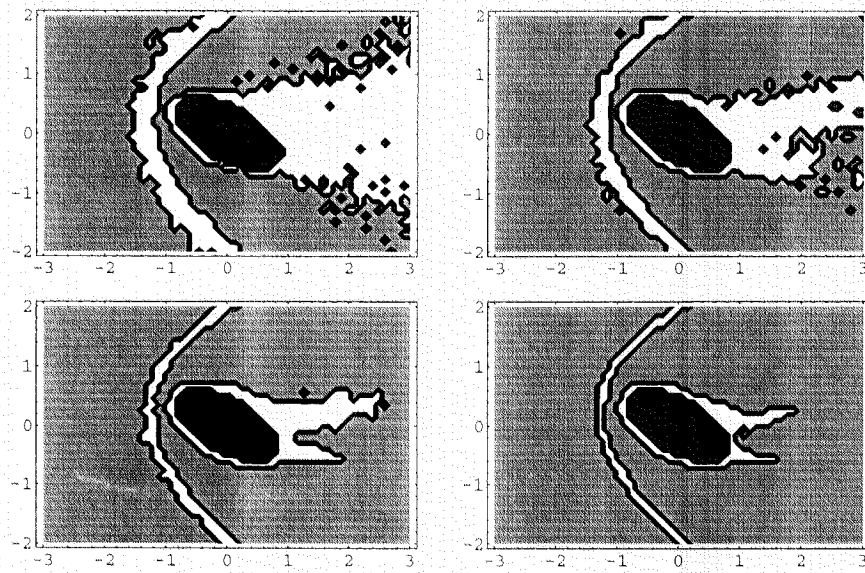


Figure 1: Boltzmann and Euler domains for mean free paths 0.1m, 0.05m, 0.025m and 0.0125m

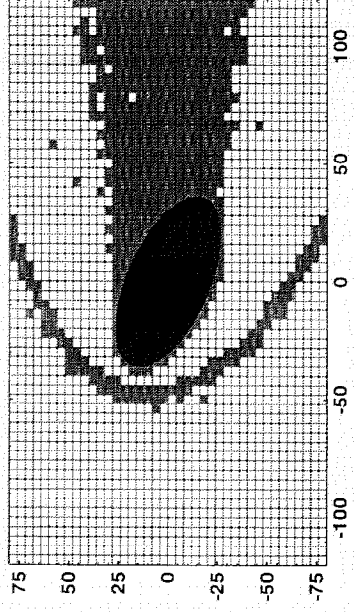


Figure 2: Grid in Boltzmann and Euler domains

mean free path (m)	Coupling procedure	Boltzmann	Euler	No. of particles
$\lambda = 0.1$	3.6	3.9	3.4	$96 \cdot 10^3$
$\lambda = 0.05$	23.7	31.6	14.4	$384 \cdot 10^3$
$\lambda = 0.025$	91.3	190.1	46.0	$1152 \cdot 10^3$
$\lambda = 0.0125$	318.4	1035.2	133.0	$3072 \cdot 10^3$

Table 1: Comparison of CPU time for coupling algorithm and full Boltzmann (Gain due to reduced time steps in the Euler domains)

in the whole domain. This yields a large gain in CPU time for these situations compared to a full Boltzmann solution.

We compute numerical solutions for mean free paths ranging from  $\lambda = 0.1\text{m}$  to  $\lambda = 0.006\text{m}$ . The results are compared with those of the pure Boltzmann and Euler code. Figures 3 and 4 show the results for the stationary state for mean free path  $0.1\text{m}$ . Figure 3 shows contour plots of density (on the left) and temperature (on the right) for pure Boltzmann code, hybrid code and pure Euler code (from above). Figure 4 shows the temperature values along the horizontal line in the middle of the computational domain. One observes here that the Euler shock is thinner than the Boltzmann shock. Using a scheme for the Euler equations, which captures the shock in a better way, this effect would have been stronger. In the following figures the mean free path is chosen as  $0.025\text{m}$ . In Figures 5 and 6 all solutions are plotted on the coarse Euler grid, although, obviously, a fine grid has to be used in the Boltzmann domain for the computation. In both cases hybrid code and full Boltzmann solver essentially yield the same results.

The time steps chosen for the Boltzmann and Euler regions are given by (8) for the Boltzmann code and the CFL condition for Euler. The spatial grid size for Boltzmann is chosen according to the mean free path. Denoting the mean free path by  $\lambda$  this leads to  $\Delta x_B = \lambda, \Delta t_B = \frac{\Delta x_B}{u_\infty}$  for Boltzmann and  $\Delta x_E = 0.1, \Delta t_E = \frac{\Delta x_E}{u_\infty}$  for the Euler region. This means that the relation between the time and space discretizations in the two domains is given by  $\Delta x_B = \frac{\Delta x_E}{s}, \Delta t_B = \frac{\Delta t_E}{s}$  with  $s = \frac{\Delta x_E}{\lambda}$ . This yields the following comparison of CPU time: In Table 1 we did note the CPU time for a full Boltzmann simulation together with the CPU time of the coupled solution and the full Euler solution. Table 1 shows the comparison for the same total number of particles in the whole computational domain. The CPU times are given in minutes.

Table 2 shows a comparison of the CPU time for a total number of particles proportional to the number of cells used in the calculation. One observes for a mean free path of  $\lambda = 0.0125\text{m}$  a gain in CPU time by a factor 13.

For mean free path  $\lambda = 0.006\text{m}$  a full Boltzmann solution is already extremely time consuming. For the coupled solution with 20 particles per cell on the average the CPU time was approximately 440 min.

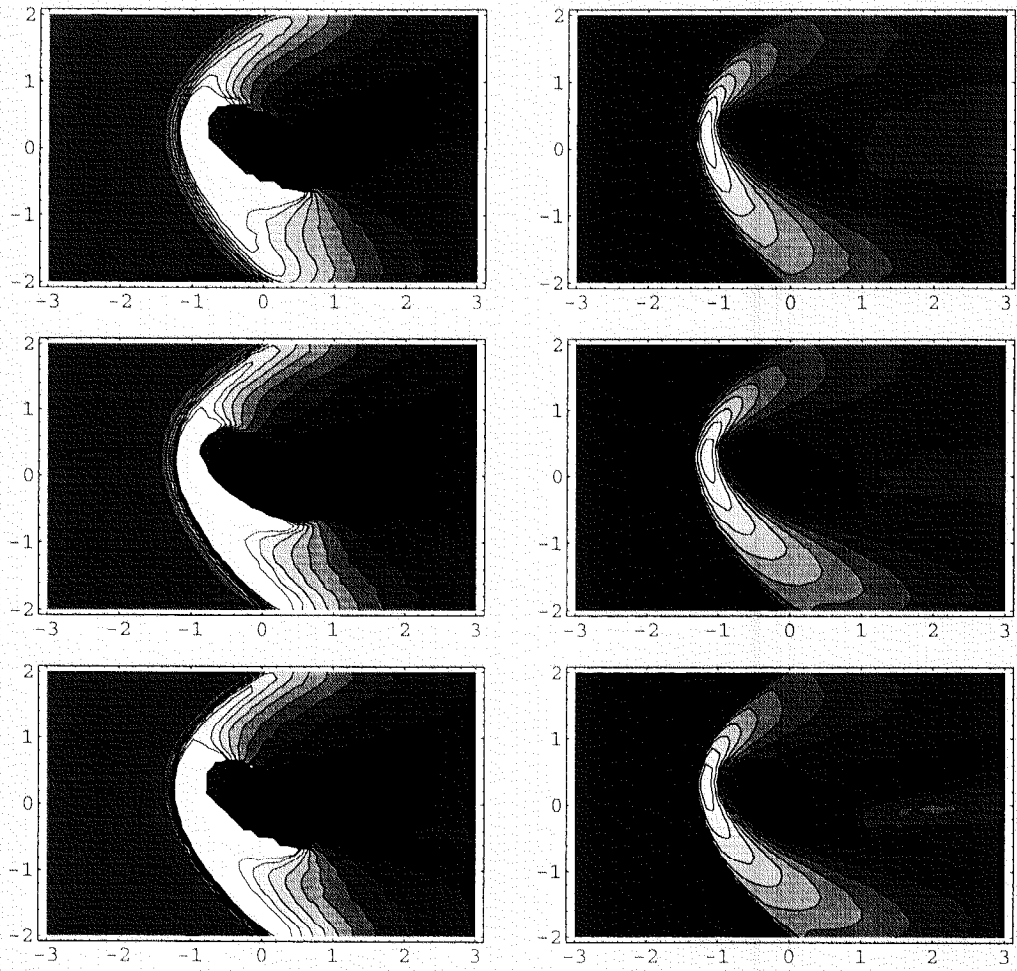


Figure 3: Contour plots for Boltzmann, hybrid and Euler codes with  $\lambda = 0.1m$



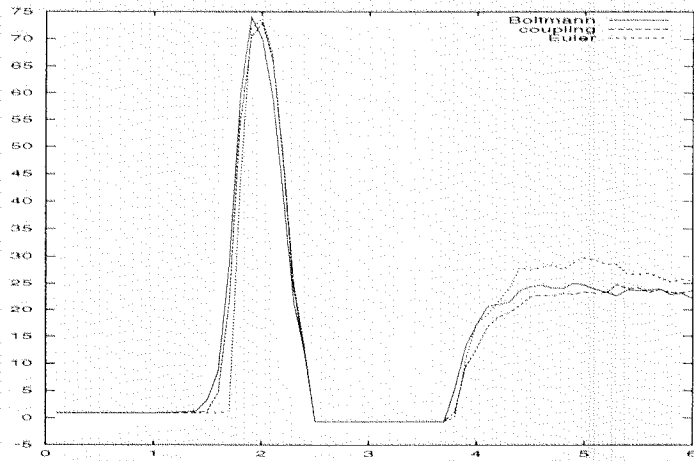


Figure 4: Temperature values for  $\lambda = 0.1m$

mean free path (m)	Coupling procedure	Boltzmann	Particles per cell
$\lambda = 0.1$	3.6	3.9	40
$\lambda = 0.05$	10.1	31.6	40
$\lambda = 0.025$	25.3	190.1	30
$\lambda = 0.0125$	79.7	1035.2	20

Table 2: Comparison of CPU time for coupling algorithm and full Boltzmann (Total gain)

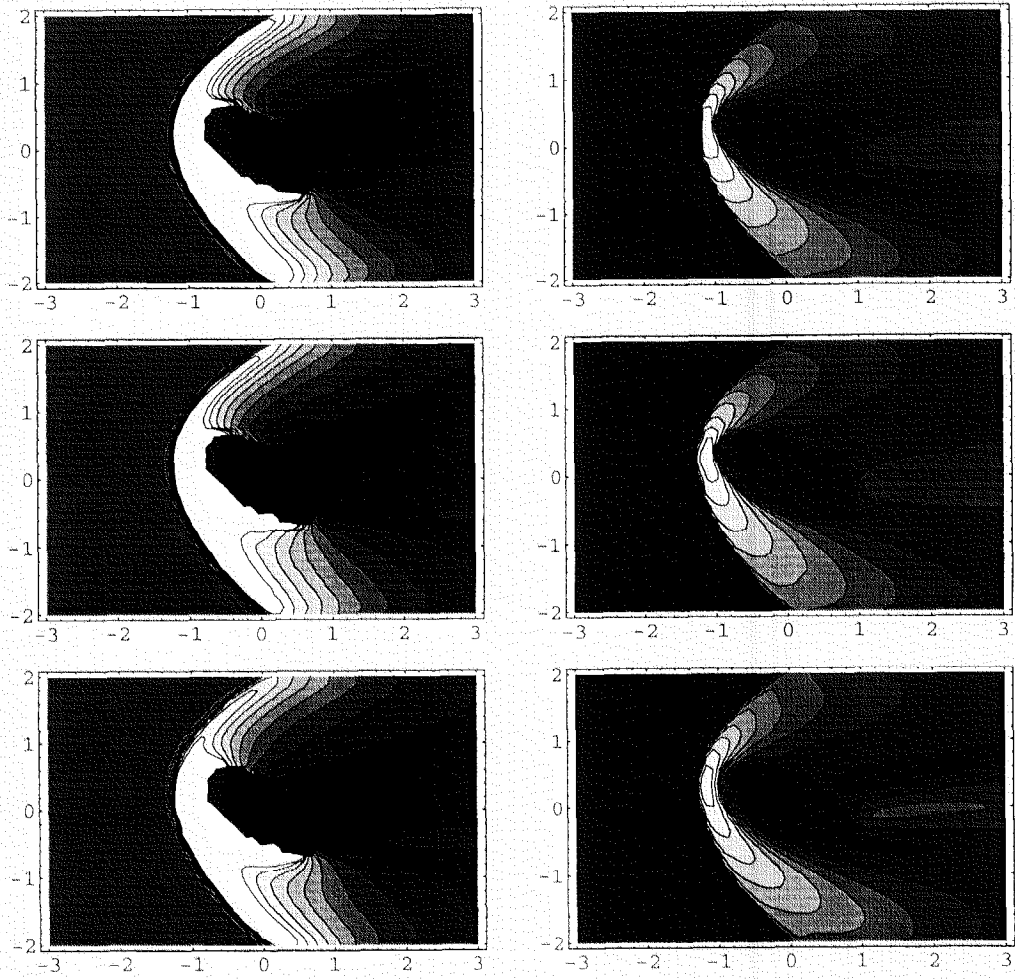


Figure 5: Contour plots for hybrid and Euler codes with  $\lambda = 0.025m$  plotted on the coarse grids

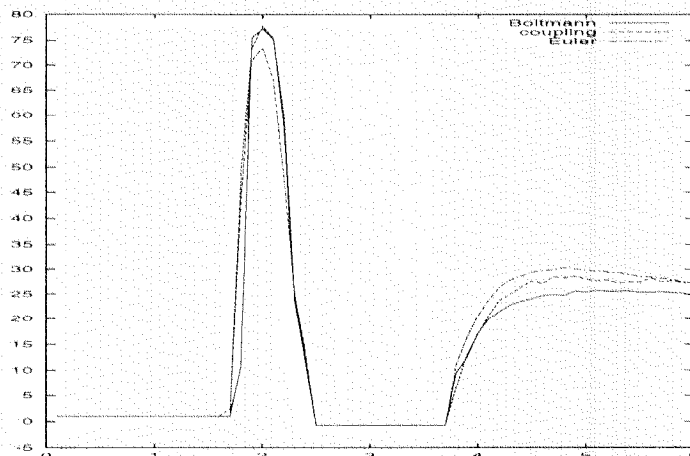


Figure 6: Temperature values for  $\lambda = 0.025\text{m}$  plotted on the coarse grid

## Conclusions

- The adaptive coupling procedure proposed in this paper is easily implemented due to the use of particle codes for Boltzmann and Euler equations.
- The domain decomposition algorithm allows a transition from large to very small Knudsen numbers.
- The gain in CPU time compared to a full Boltzmann solution is considerably using time steps and spatial discretizations appropriate to the problem
- Although standard codes for the Euler equations are faster than the above particle method, such a method is most appropriate for a coupling procedure like the one presented in this work.

### Acknowledgements:

This work was supported by a grant from 'Deutscher Akademischer Austauschdienst' (DAAD). We are grateful to Helmut Neunzert and Sergeij Rjasanow for interesting and helpful discussions.

## References

- [1] H. Babovsky. A convergence proof for Nanbu's Boltzmann simulation scheme. *Eur. J. Mech., B*, 8:41, 1989.
- [2] H. Babovsky and R. Illner. A convergence proof for Nanbu's simulation method for the full Boltzmann equation. *SIAM J. of Num. Anal.*, 26:45, 1989.

- [3] G.A. Bird. *Molecular gas dynamics*. Clarendon Press, Oxford, 1976.
- [4] J.F. Bourgat, P. Le Tallec, F. Mallinger, B. Perthame, and Y. Qiu. Coupling Boltzmann and Euler equations without overlapping. *preprint, INRIA, Paris*, 1991.
- [5] J.F. Bourgat, P. Le Tallec, D. Tidriri, and Y. Qiu. Numerical coupling of nonconservative or kinetic models with the conservative compressible Navier-Stokes equations. In *Fifth International Symposium on Domain Decomposition methods for P.D.E.*, SIAM, Philadelphia, 1991.
- [6] I.D. Boyd, G. Chen, and G.V. Candler. Predicting failure of the continuum fluid equations in transitional hypersonic flows. *AIAA*, 94:2352, 1994.
- [7] R. Caflisch. The fluid dynamical limit of the nonlinear Boltzmann equation. *CPAM*, 33:651, 1980.
- [8] C Cercignani. *The Boltzmann Equation and its Applications*. Springer, 1988.
- [9] C. Cercignani, R. Illner, and M. Pulvirenti. *The Mathematical Theory of Dilute Gases*. Springer, 1994.
- [10] S.M. Deshpande. A second order accurate kinetic theory based method for inviscid compressible flows. *Tec. Paper, NASA-Langley Research Center*, 2613, 1986.
- [11] U. Giering. *Matching of Kinetic and Aerodynamics equations*. PhD Thesis, Kaiserslautern, 1995.
- [12] H. Grad. On the kinetic theory of rarefied gases. *CPAM*, 2:331, 1949.
- [13] F. Gropengiesser. *Gebietszerlegung bei Strömungen im Übergangsbereich zwischen Kinetischer Theorie und Aerodynamik*. PhD Thesis, Kaiserslautern, 1991.
- [14] R. Illner and H. Neunzert. Domain decomposition: Linking kinetic and aerodynamic descriptions. *AGTM preprint, Kaiserslautern*, 90, 1993.
- [15] M. Junk, A. Klar, J. Struckmeier, and S. Tiwari. Particle methods for evolution equations. *preprint, Kaiserslautern*, 1996.
- [16] S. Kaniel. A kinetic model for the compressible flow equations. *Indiana University Mathematics Journal*, 37:537, 1988.
- [17] A. Klar. Asymptotic-induced domain decomposition methods for kinetic and drift diffusion semiconductor equations. *to appear in SIAM J. Sci. Comp.*
- [18] A. Klar. Domain decomposition for kinetic problems with nonequilibrium states. *Eur. J. Mech./B Fluids*, 15:203, 1996.

- [19] H.J. Kreuzer. *Nonequilibrium Thermodynamics and its Statistical Foundation*. Clarendon, Oxford, 1981.
- [20] H. W. Liepmann, R. Narasimha, and M.T. Chahine. Structure of a plane shock layer. *Phys. Fluids*, 5:1313, 1962.
- [21] A. Lukschin, H. Neunzert, and J. Struckmeier. Coupling of Boltzmann and Navier Stokes equations. *Interim Report for the Hermes Project*, DPH 6174/91, 1992.
- [22] J. Meixner. Zur Thermodynamik der irreversiblen Prozesse. *Z. Phys. Chem. B*, 53:253, 1941.
- [23] H. Neunzert and J. Struckmeier. Particle methods for the Boltzmann equation. *Acta Numerica*, page 417, 1995.
- [24] B. Perthame. Second-order Boltzmann schemes for compressible Euler equations in one and two space dimensions. *SIAM J. Numer. Anal.*, 29:1, 1992.
- [25] W. Schreiner. *Partikelverfahren für Kinetische Schemata zu den Eulergleichungen*. PhD Thesis, Kaiserslautern, 1994.
- [26] S. Tiwari. Coupling of Boltzmann and Euler equations with automatic domain decomposition. *preprint, Kaiserslautern*, 1997.
- [27] S. Tiwari. *Domain Decomposition in Particle Methods for Boltzmann and Euler equations*. PhD Thesis, Kaiserslautern, 1998.
- [28] S. Tiwari and S. Rjasanow. Sobolev norm as a criteria of local thermal equilibrium. *to appear in Eur. J. Mech. B/Fluids*.